Downstream rounding rate of pebbles in the Himalaya

Prakash Pokhrel[1,2], Mikael Attal[1], Hugh D. Sinclair[1], Simon M. Mudd[1], and Mark Naylor[1]

[1]School of GeoSciences, University of Edinburgh, UK
[2]Department of Mines and Geology, Nepal

Correspondence: Prakash Pokhrel (pokhrel.prakash@ed.ac.uk)

Abstract. Sediment grains are progressively rounded during their transport down a river. For more than a century, Earth scientists have used the roundness of pebbles within modern sediment, and of clasts within conglomerates, as a key metric to constrain the sediment's transport history and source area(s). However, the current practices of assessment of pebble roundness are mainly qualitative and based on time consuming manual measurement methods. This qualitative judgement provides the transport history only in a broad sense, such as classifying distance as 'near' or 'far'. In this study, we propose a new model that quantifies the relationship between roundness and the transport distance. We demonstrate that this model can be applied to the clasts of multiple lithologies including modern sediment as well as conglomerates deposited by ancient river systems. We present field data from two Himalayan catchments in Nepal. We use the Normalized Isoperimetric Ratio (IR_n) which relates a pebble's area (A) to its perimeter (P), to quantify roundness. The maximum analytical value for IR_n is 1, and IR_n is expected to increase with transport distance. We propose a non-linear roundness model based on our field data, whereby the difference between a grain's IR_n and the maximum value of 1 decays exponentially with transport distance, mirroring Sternberg's model of mass loss or size reduction by abrasion. This roundness model predicts an asymptotic behaviour for IR_n, and the distance over which IR_n approaches the asymptote is controlled by a rounding coefficient. Our field data suggest that the roundness coefficient for granite pebbles is eight times that of quartzite pebbles. Using this model, we reconstruct the transport history of a Pliocene paleo-river deposit preserved at the base of the Kathmandu intermontane Basin. These results, along with other sedimentary evidence, imply that the paleo-river was much longer than the length of the Kathmandu Basin, and that it must have lost its headwaters through drainage capture. We further explore the extreme rounding of clasts from Miocene conglomerate of the Siwaliks Zone and find evidence of sediment recycling.

1 Introduction

1.1 A brief history of shape indices

The rounding of pebbles found within conglomerates has long been linked to abrasion that occurs prior to deposition as pebbles are transported by rivers, with greater rounding being typically associated with increased transport distance (Mills, 1979; Russell, 1980; Lindsey et al., 2007; Yingst et al., 2016). This also applies to modern rivers: the shape of pebbles has been used to locate sediment sources and define the control exerted by hydraulic transport on abrasion processes (Wentworth, 1919; Lindsey et al., 2005; Domokos et al., 2009; Litty and Schlunegger, 2017; Gale, 2021). The use of pebble roundness is not limited to

Earth: research on Mars has connected roundness to both the existence of ancient river networks as well as the transport history of Martian sediments (Yingst et al., 2008; Jerolmack, 2013; Williams et al., 2013; Szabo et al., 2015). Several researchers have attempted to relate pebble roundness with sediment transport distance based on field measurements (Wentworth, 1922; Mills, 1979; Roussillon et al., 2009; Litty and Schlunegger, 2017) as well as laboratory experiments (Wentworth, 1919; Abbott and

30 Peterson, 1978).

The morphology of sediment grains plucked from bedrock, sourced from hillslopes and/or re-worked from existing deposits gets modified as the grains are transported downstream (McPherson, 1971). It is known that shape, size, and roundness evolve mainly due to abrasion processes that have acted upon the pebble in time and space (Brewer and Lewin, 1993). Abrasion processes like sand blasting, chipping and granular removal by crushing or grinding will increase roundness, whereas chipping

35 of large fragments, cracking and subsequent fracturing will decrease it (Brewer and Lewin, 1993). All of these processes act on sediment grains while they are being carried by water current in rivers, leading to a reduction of their size and alteration of their shape. Researchers have evidenced a general relationship between roundness and attrition of sediment transported as bedload in rivers (Novák-Szabó et al., 2018). They also showed that the effectiveness of attrition/abrasion varies with the lithology of the clasts (Attal and Lave, 2009). For instance, the varied grade of weathering of a source rock prior to its introduction as

40 sediment into the fluvial environment can lead to varied degrees of roundness for the same transport distance (Gale, 2021). It is also possible to discriminate between sediment shaped on a beach, in a river and or a sub-marine fan by using shape indices (Howard, 1992). Hence, roundness, together with other evidence, is a powerful tool for provenance analyses in sedimentary basins (Lindsey et al., 2007).

Although shape is a fundamental property for all kind of objects, including sediments, it remains one of the most difficult

45 to characterize and quantify (Wentworth, 1933; Barrett, 1980; Blott and Pye, 2008). Different terms such as 'form' (Sneed and Folk, 1958), 'roundness' (Wentworth, 1922, 1923), 'sphericity' (Wadell, 1935) and 'irregularity' (Blott and Pye, 2008) are most commonly used to define the shape of sediment particles. The term sphericity is often used synonymously with roundness. Wadell (1935) first proposed the term sphericity, which represents the degree to which a particle approximates the shape of a sphere, and is independent of its size. In contrast, roundness refers to the sharpness of pebble edges (Cruz-Matías et al., 2019).

50 Even though the concepts of roundness and sphericity are related, they are two distinct terms. For example, an object with a regular dodecahedron shape has a high degree of sphericity but has very low roundness (Blott and Pye, 2008). There are numerous methods available for the calculation of roundness, with new methods still being proposed and old methods falling out of favour. Some earlier definition of roundness include: the ratio of the radius of curvature of the sharpest corner to the mean radius of the particle (Wentworth, 1922), the ratio of the diameter of curvature of the sharpest corner to the intermediate

55 axis of grain (Kuenen, 1956), the ratio of the diameter of curvature of the sharpest corner to the diameter of the largest inscribed circle (Dobkins and Folk, 1970), as well as indices based on the ratio of a pebble's perimeter to its area in 2D (Roussillon et al., 2009), to name only a subset of previously applied metrics.

1.2 Measurement of shape indices: technological advances and challenges

Many studies are either based on direct measurements in the field (Wentworth, 1922, 1923; Litty and Schlunegger, 2017) or
60 the manual tracing of outline of pebbles using the 2D images (Quick et al., 2019). Both of these methods are subject to human
bias and are almost impossible to replicate. However, studies developing an automated workflow to reduce the subjectivity
in calculating the shape parameters have been recently published. For example, Roussillon et al. (2009) developed a tool
for the automatic extraction of pebble shape from 2D images. Similarly, Cassel et al. (2018) assessed and validated the use
of an automated toolbox to define the relation between roundness metric trends and abrasion using the 2D images. Tunwal
65 et al. (2020) proposed image-based automated particle shape analyses for both consolidated and loose sediments which can
measure traditional, mathematically complex and common geometric shape parameters. Fehér et al. (2020) demonstrated the
effectiveness of 3D laser scanning of beach pebbles by comparing the results with a hand-measured set of pebbles. Thus,
advances in technology are making automatic extraction of shape parameters possible. Automated image analysis and Fourier
grain shape analysis allow modern workers to analyse a high volume of roundness metrics quickly and easily (Diepenbroek
70 et al., 1992).

However, while a good method should have a high degree of reproducibility, the choice of an appropriate roundness metric
is still based on the judgement of authors, leading to difficulties when comparing results from different studies (Barrett, 1980;
Diepenbroek et al., 1992). To address this problem, some researchers (Roussillon et al., 2009; Purinton and Bookhagen, 2019)
have developed automated methods to extract multiple indices characterizing a pebble's shape and size, which facilitates com-
75 parison and correlation of roundness indices obtained using different methods. For instance, Roussillon et al. (2009) compared
a series of geometric parameters that characterize roundness, such as Wadell (1935)'s roundness index (r_w), Durian et al.
(2006)'s roundness index (r_d) and Cottet (2006)'s roundness index (r_p) along with the pebbles' axial ratio (a/b), circularity
and convexity. What these studies showed is that even with automated methods, the above indices are sensitive to the method
of assessments.

80 Cassel et al. (2018) explored the effect of pebble position, image resolution and enhancement on the indices of roundness
and shape measurements in which the outline of pebbles is extracted from 2D images using the automated tool developed by
Roussillon et al. (2009). Indices such as r_p, convexity and circularity were found to be more powerful than r_w to assess round-
ness (Roussillon et al., 2009). However, indices r_p and r_d were found to have different sensitivities to the picture resolution and
enhancement. Cassel et al. (2018) also described miss-classification of pixels due to the shadowing effect, the bleeding effect
85 (dark pixels influenced by adjacent red or background clear colour pixels), and the overexposure effect (shining pixels). Such
effects may deteriorate the quality of measurements obtained using automated 2D image processing. Durian et al. (2006) found
that the curvature measured along the contour of pebbles allows finer discrimination of a pebble's shape than the traditional
measures of aspect ratio. Hence, circularity appears to be the best choice to measure pebble roundness when the outline of
a pebble is extracted using 2D image processing. A series of recent studies have used the 'Isoperimetric Ratio', a parameter
90 equivalent to circularity, to measure the downstream evolution of pebble roundness in the fluvial environment on Mars (Szabo
et al., 2015) and in the Himalaya (Quick et al., 2019), rather than the axial ratio of pebbles.

1.3 Controls on pebble shape: consensus and debates

There are different views regarding the controls on and trends in pebble roundness as one moves downstream (Figure 1). Wentworth (1922) studied the relationship between pebble shape and flow distance based on roundness ratio and flatness ratio using field and laboratory measurements, and suggested the rounding effect of abrasion diminishes downstream. Additionally, they noticed a strong correlation between field measurements and an experimentally-derived curve. Field-measured roundness shows a systematic trend, i.e., an increase in rounding with distance downstream, in the upstream part of catchments where there is no contribution of more angular pebbles from lateral tributaries (Brewer and Lewin, 1993; Roussillon et al., 2009). Similarly, a two-phase evolution of pebble shape was proposed by Miller et al. (2014) based on theory and measurements or pebble roundness along a river in Puerto Rico: in the first phase (headwaters), pebbles are rapidly rounded, while in the second phase (downstream part of the river system), pebbles are reduced in size with little changes in roundness. While Roussillon et al. (2009) argue that the roundness trends can persist over long distances (at least 20-50 km) and disagree with the idea that roundness changes are limited to the upmost part of the fluvial network, all these studies (Roussillon et al., 2009; Wentworth, 1922; Vanbrabant et al., 1998; Miller et al., 2014) suggest a non-linear relationship between transport distance and roundness: grains round rapidly in the first part of their journey through the fluvial system, and this rounding slows down further downstream.

Although the three parameters - shape, size and roundness - are usually associated with each other, there is debate about how they co-evolve and whether some of them control the others (Domokos et al., 2014). The downstream evolution of a pebble's shape and roundness has been showed to be controlled by the initial grain size, hardness and existence of fabrics within (Kuenen, 1956; Lindsey et al., 2005), with some of these factors directly related to the lithology of the pebble itself (Kuenen, 1956; Sneed and Folk, 1958). For example, pebbles of limestone and andesite achieve their maximum roundness after only a few kilometres of transport distance, whereas rocks with high silica content like chert and quartzite can still have low relative roundness after tens of kilometres of transport (Sneed and Folk, 1958). Kodama (1994) also noticed that chert and andesite pebbles were reduced in size by different abrasion processes in the Watarase River in Japan, which affected the grain size distribution of these lithologies and will likely influence how they pebbles round. Due to the brittle nature of high silica content rocks, roundness may not change or may even decrease during transport because of spallation, chipping or fracturing (Sneed and Folk, 1958). This may also happen in polycrystalline rocks like pegmatite (igneous rocks with mineral grain > 5 cm) due to physical breakage along large grain boundaries during transport (Lindsey et al., 2005).

A study in an Alpine river also showed that the water discharge and flow strength don't exert the main control on the shape and size of fluvial pebbles (Litty and Schlunegger, 2017). Instead, the lithological composition of the pebbles itself, and therefore that of the sediment supplied to the river through mass failure, was the key determining factor on the pebble shape and roundness (Litty and Schlunegger, 2017). This result is consistent with the study by Attal and Lave (2009) who designed a circular flume to replicate the abrasion processes effective during vigorous fluvial transport in powerful Himalayan rivers during the monsoon (Attal et al., 2006): while the experiments at high flow velocities caused widespread pebble breakage leading to abrasion rates an order of magnitude greater than previously published, breakage did affect mostly schist and sandstone

pebbles (Attal and Lave, 2009). Abrasion rates for other lithologies such as granite, gneiss and limestone remained comparable to previously published results, consistent with field observations (Attal and Lave, 2006).

1.4 Motivation

This study has a methodological aim and a research-focused aim. It provides a methodology for the measurement of pebble roundness, which is automatic, time efficient, and provides results that can be replicated when applied to the same image. While Roussillon et al. (2009) and Cassel et al. (2018) describe automatic methods of pebble shape analysis using 2D images, we provide additional information on site location, pebble collection and photography, as well as details about an image processing technique using an open access graphics user interface (GUI) software (Schneider et al., 2012). We present a workflow to help researchers replicate results and adopt this technique in future studies. The method also allows the manual correction of overexposure, shadowing, wet pebble and bleeding effects described by Cassel et al. (2018). We use the Isoperimetric Ratio as the geometric parameter to characterize a pebble's roundness, building on previous recent studies (Miller et al., 2014; Szabo et al., 2015; Quick et al., 2019). We further explore the use of a Normalized Isoperimetric ratio (IR_n) first developed by Quick et al. (2019). Based on measurements in two Himalayan catchments with varied rock types and provenance settings, we propose a new model to relate the roundness (IR_n) with the transport distance (d), that is, the distance travelled by the pebbles from their entrance point in the river system to the location where they were measured. We further explore the applicability of our roundness-distance relationships to estimate the distance travelled by Miocene and Pliocene sediments in Himalaya.
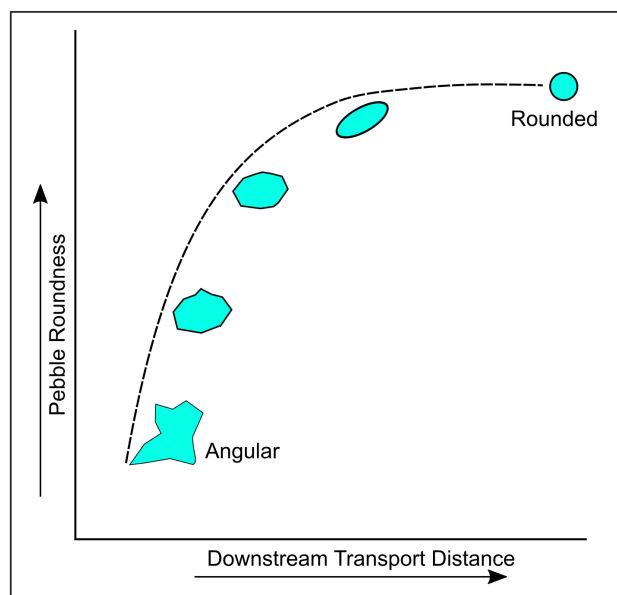
Figure 1. Schematic diagram showing the downstream shape and size changes of a particle as it is transported downstream along a river. An angular pebble becomes rounded after travelling a certain distance along the river. Note that this diagram shows a conceptual model in which the relationship between roundness and transport distance is non-linear, as suggested by previous studies (see text for discussion).

2 Materials and Methods

In this section, we describe the shape index chosen in this study, as well as a complete workflow for the field data collection, image processing and data analysis, including the description of the study catchments and collection strategy.

145 ### 2.1 Choice of shape index

As mentioned in the introduction section (Sect. 1.1 and 1.2), many shape indicators exist. The parameter used in this study to define pebble roundness is similar to the term 'roundness' first proposed by Cox (1927) (using a different name) which is defined as the ratio of the area (A) of a pebble in 2D to its perimeter (P), as shown in Equation 1 (Blott and Pye, 2008). The theoretical value of the 'Isoperimetric Ratio (IR)' varies between 0 and 1; a perfect circle (perfectly spherical pebble) will have

150 a value of 1, with measured IR values for the pebbles typically ranging from 0.5 to 1.0 (Quick et al., 2019).

$$IR = (4\pi A)/P^2 \tag{1}$$

However, Roussillon et al. (2009) and Quick et al. (2019) found that IR is sensitive to both elongation and roundness. For instance, a perfectly rounded elliptic pebble with an axis ratio b/a of 0.5 (where a and b are the longest and shortest axes in the plan considered, respectively) will have an IR of 0.84, which could be similar to that of a more angular but "spherical" pebble

155 ($b/a = 1$) (Quick et al., 2019). Quick et al. (2019) found that the maximum IR a pebble can achieve decreases with decreasing axis ratio. They developed a 'Normalized Isoperimetric Ratio' (IR_n) designed to remove any dependency on elongation, and only measure the angularity (or roundness) component from the IR (Equation 2). The normalized isoperimetric ratio (IR_n) is calculated by dividing IR by the maximum theoretical isoperimetric ratio a pebble can achieve based on its measured axis ratio (IR_t). Here, we use the Ramanujan approximation (Villarino, 2005) to calculate the area and perimeter of an ellipse of axes a

160 and b for the calculation of the maximum theoretical isoperimetric ratio (Equation 3).

$$IR_n = IR/IR_t \tag{2}$$

$$IR_t = \pi(a+b)(1 + (3h/(10 + (4 - 3h)^{1/2}))) \tag{3}$$

where

$$h = (a-b)^2/(a+b)^2 \tag{4}$$

165 Our subsequent analyses use IR_n which removes the effect of elongation and gives the true measure of roundness of the pebbles.

2.2 Study catchment and site selection

Our aim in this study is to quantify the degree to which pebbles round as they travel downstream. It is therefore essential to select catchments where an identifiable lithology is only supplied from one portion of the catchment so we can be confident
170 rounding measurements taken as a function of travel distance are not confounded by addition of less rounded clasts of the same lithology further downstream. We have identified two catchments that meet this criterion, from which our samples are drawn. The catchments lie in western and central Nepal and their rivers are the Banganga River and Rapti River, respectively (Figure 2). Both of these catchments have headwaters in Lower/Lesser Himalayan lithologies; neither are connected to large trans-Himalayan rivers upstream of our sampling areas.

175 The Banganga River contains two thick ($\sim$100 m) quartzite units near the headwaters of the catchment. The remainder of the catchment consists of Precambrian-Paleozoic meta-sedimentary rocks and Eocene-Pleistocene sedimentary rocks (Sakai, 1983; Dhital, 2015). Unlike many locations along the Himalayan mountain front, there are no molasse conglomerates that may input recycled pebbles into the river (Quick et al., 2019). Thus the Banganga River is perfectly suited for studying the rounding of quartzite pebbles over a known distance from their source.

180 The Rapti River catchment comprises an exposed granite body in its headwaters, and so is suited to measuring the progressive rounding of granite pebbles downstream from their source (Figure 2(d)). Although this catchment includes outcropping quartzite and granite, quartzite bands are exposed in a number of downstream locations. Moreover, conglomerate beds of Upper Siwaliks are also exposed in the southernmost part of this catchment, and so recycling may be an issue (Quick et al., 2019). Hence, we only consider granite pebbles for the roundness analysis to avoid multiple sources and recycled pebbles of quartzite
185 in the modern sediment of the Rapti River.

At first, sites for the pebble collection were identified using open access global base maps (Google Map and Google Earth). Where possible, we aimed to have relatively uniform spacing in terms of downstream flow distance between sampling sites. Some variation in sampling distance along the river does occur, due to site accessibility.

The quartzite pebbles were collected at twelve locations on the Banganga River and granite pebbles were collected from
190 five locations on the Rapti River. The location of each sampling site is shown in Figure 2. We extracted flow distance from the channel head using the LSDTopoTools software Mudd et al. (2022). We then compared the normalized isoperimetric ratio against flow distance for our samples. The total distance covered by the pebble collection along the river is $\sim$50 km in each catchment. We only sampled active gravel bars from the main channel, and we avoided gravel bars with any evidence of human influence. The most common influences observed in the field were mounds of clasts indicative of mining for aggregate, and
195 construction of temporary diversions or access roads along and across the river channel. Additionally, we did not sample gravel bars close to landslides.

2.3 Pebble Collection and photography in the field

The Banganga River covers the part of synclinorium in western Nepal mapped by Sakai (1983). This catchment includes quartzite bands exposed at two locations towards the channel head. Downstream from the lower quartzite band, only shale,
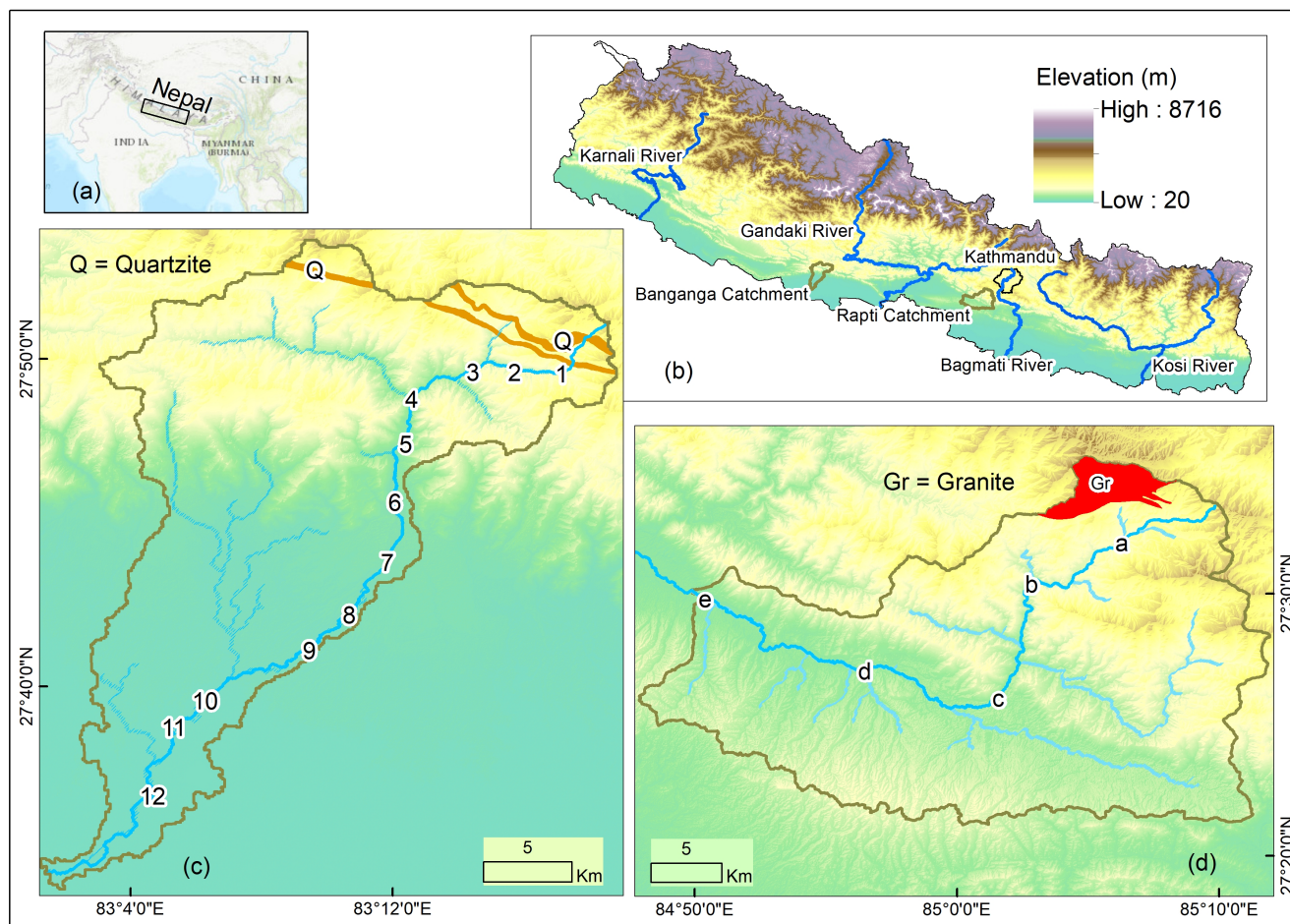
Figure 2. Location map. **a**: Location of the Himalayas and Nepal. **b**: Political boundary of Nepal with the location of river catchments used for sample collection. **c** and **d**: study catchments and river networks showing the location of each sample site and bedrock exposure area for the lihtology of the pebble collected in the field along the Banganga River (**c**) and Rapti River (**d**). Note: 1, 2, ..., 12 in (**c**) are the sample sites for quartzite pebbles and a, b, ..., e in (**d**) are the samples sites for granite pebbles. In both catchments, transport distance to each sample site is calculated from the channel head using Mudd et al. (2022). Data source: Global map- ESRI Basemap, Topographic data-open topography ALOS World 3D (Japan Aerospace Exploration Agency, 2021), Political boundary of Nepal and rivers- Department of Survey-Nepal, Lithological boundaries- Sakai (1983) and Department of Mines and Geology (2011).

.

200 limestone, dolomite, sandstone, mudstone and siltstone are exposed. The quartzite bands are competent and white to grey in colour, and are the source of boulders, cobbles and pebbles that can be distinguished in gravel bars several kilometres downstream. This area lacks granite in the source region, so only the pebbles of quartzite rock are collected from this catchment. We used 10% dilute Hydro-chloride acid (HCl) to differentiate the pebbles sourced from greyish siliceous carbonate rocks

(limestone and dolomite) from those derived from quartzite. We carefully examined pebbles based on texture and mineralogy
205 using a hand lens, thus we are confident all our sampled pebbles in the Banganga River are indeed quartzite and not some other
rock type.

We applied a similar sampling procedure in the Rapti catchment, south of the Kathmandu. In the Rapti, we sampled granite
pebbles rather than quartzite, as explained in Sect. 2.2. The field identification of granite pebbles is easier than identification of
quartzite pebbles as there are no other rocks with igneous texture exposed in this study catchment. The location of the quartzite
210 band in the Banganga catchment, and the granitic body in the Rapti catchment, are shown in Figure 2.

Upon arriving at a potential sampling site, we first assessed whether the gravel bar was close to the active channel (i.e., not
a terrace) and not influenced by human activities. We then extended a 25 m linear transect along the gravel bar and sampled all
pebbles of quartzite and/or granite that could be lifted manually by both hands. In upstream regions, close to the channel head,
we found it difficult to find enough grains of a size that could be lifted from the gravel bar. Therefore, multiple (a maximum of
215 three) 25 m transects were used for the pebble collection in sampling locations with very coarse (up to boulder size) sediments.
To minimise the bias in sample collection, only the pebbles from a single gravel bar were collected at each sampling site. We
aimed to collect approximately 100 quartzite pebbles and 30 granite pebbles at each site but there were sites where we collected
fewer than 100. In total, we collected and photographed about 2000 pebbles in the field.

Our method requires imaging the pebbles to extract their outlines, so we needed a method of collecting high contrast images
220 in the field. Studies have attempted to collect similar images. For example Cassel et al. (2018) used a flat surface of 1 m^2
with a red background to photograph the pebbles in the field. Here, we covered a rigid board with a black blanket and used
this surface to photograph the pebbles. We placed pebbles along their longest and intermediate axes (covering the maximum
surface area). We then held a camera directly above the surface at chest height, and took a photograph of the pebbles in a scene
that included a scale of known dimension. We used a large umbrella to prevent the photographed surface from being exposed
225 to direct sunlight. This eliminates the shadow of pebbles and mitigates any reflecting surfaces of multi-coloured mineral grains
within the granitic pebbles. We took care to remove dust particles and any other field dirt from the flat surface.

2.4 Image Processing

Many previous studies of pebble roundness are based on manual digitisation of pebble outlines from photographs of gravel bars
(Quick et al., 2019; Miller et al., 2014). The results from manual tracing are difficult to replicate and uncertainties are introduced
230 because of personal judgement. Additionally, manual tracing is a time consuming process. We used image processing to
circumvent these issues. Our processing workflow uses the open access software ImageJ (Schneider et al., 2012) (Figure 3).

Our workflow extracts the area (A), perimeter (P), the length of the major axis (a) and minor axis (b) using the automatic
digitisation of a pebble's outline. There are challenges to automate the pebble extraction process including the overexposure,
shadowing, wet pebble and bleeding effects in the 2D images of pebble (Cassel et al., 2018). Hence, the automated outline
235 extraction demands a multi-stage technique to measure the geometric parameters of pebble roundness from the 2D images
(Figure 3).
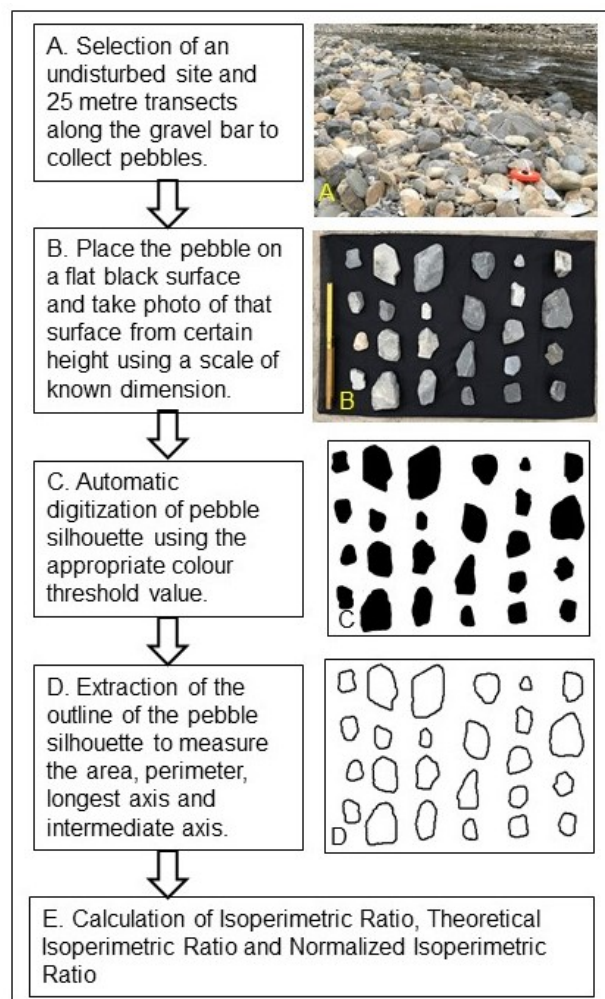
Figure 3. Flow chart showing the work flow for the site selection, pebble collection, photography technique, image processing and calculations.

The basic principle of our automatic method is to read the pebble silhouette automatically by a software using a colour threshold. The colour threshold value differentiates the black background and the pebble area. After this step, we removed the background surface and the pebble's outline was extracted to measure the geometric parameters. Roundness values vary with the orientation of the object in a raster environment: indeed, an image in a raster will have pixelated contours, and a line that is oriented NW-SE will be 1.4 times longer than the same line oriented N-S, due to the tracing of the line following the pixel contours and adding distance when the line is not perfectly oriented in the direction of the grid (N-S or E-W); this occurs irrespective of the resolution. We address this issue by converting the pebble outline from 2D image raster to the vector format. We also perform a smoothing of the pixel boundaries while converting the pixel outline into a vector outline. The smoothing

is done in such a way that the polygons contain a minimum number of segments while remaining as close as possible to the original raster cell edges. The methodology that we adopt for the 2D image processing using the ImageJ and ArcGIS is described in detail as below:

To convert 2D field photographs (from Sect. 2.3) into pixels, open an image in ImageJ and convert it to an 8-bit type image. Use the "set scale" option by drawing a line along the object of known dimension and providing the dimension with a unit. Then adjust the image based on the threshold value using "Adjust threshold". This is an important step that extracts the shape of the pebbles by separating the pixels into foreground (object of interest - pebbles) and background (everything else). After adjusting the threshold value, the image updates in real-time to show the pixels included in the foreground and background. The image is then converted into a binary image and the 'Fill hole' option is applied to fill any holes or gaps in the foreground objects.

Once a satisfactory binary image is created in ImageJ, export the image as a geotif file that can be imported in GIS environments. To measure the area, shape, longest axis, and intermediate axis, open the geotif image in ArcGIS and provide a reference in the meter system. Then use "Raster calculator" to convert the geotif image into a raster integer file, which allows opening of the attribute table of the raster file. Open the attribute table, add a field (e.g., "pebble-shape") and assign 1 for the pixels comprising pebbles and 0 for the background pixels. Then save and stop editing.

Next, use the "Raster to polygon" conversion tool to convert the raster file into vector format, selecting the "pebble-shape" column in the value field that was added earlier. Also, select the "Simplify polygon" option to eliminate the pixelisation effect in the area and perimeter measurements. This step creates the polygon for the pebble shape, and the area and perimeter of the shape are calculated using the "calculate geometry" function in the attribute table. Finally, the major (a) axis and intermediate (b) axis are measured using the "Minimum bonding geometry" function from the search box tool in ArcGIS, with "Geometry type" as convex hull and "Geometry characteristics" as attribute added. This step provides all the measurements necessary to calculate the parameter used as a measure of roundness in this study.

3 Results

3.1 Downstream Changes in Roundness and New Roundness Model

We calculate IR_n for each pebble from all locations for the quartzite and granite pebbles (see box plot in Figure 4a for granite pebbles and Figure 4b for quartzite pebbles). The range of IR_n values is greater in the upstream sites than in downstream sites, in particular for the granite pebbles. Each location consists of a mix of angular to rounded pebbles. For example, at the upstream sites there are a small number of pebbles that are as round as pebbles that have travelled ~ 50 km downstream. Because each site has a mixture of roundness values, we have calculated five different percentiles to capture the range of and changes in IR_n at each site ($5^{th}, 25^{th}, 50^{th}, 75^{th}$ and 95th percentiles). These percentiles represent the angular to rounded sub-populations of pebbles from each location. The IR_n value of the 5th percentile represents the most angular pebbles and the 95th percentile represents the most rounded pebbles in that particular location.

As an exploratory analysis step, we applied a linear regression to each set of percentile data as a function of downstream flow distance (Figure 4c and d): while we expect IR_n to display an asymptotic behaviour towards $IR_n = 1$, we find that the trends can be reasonably approximated by linear fits over distances of $\sim$50 km. All trends show that the roundness of every
280 percentile, including the median, increases downstream (Figure 4c and d). Granite pebbles are also rounder than quartzite ones when comparing the percentiles across lithologies.

We make two key observations, that support the development of our new rounding model:

- Granite pebbles are rounder than quartzite ones when comparing the percentiles across lithologies.

- The linear fits of all percentiles have a comparable slope for the quartzite pebbles, but the slope decreases rapidly with
285 increasing percentile (that is, slope is lower for the most rounded populations as IR_n approaches 1) for the granite pebbles.

If we make the assumption that it is impossible for a given pebble to round downstream faster than another (i.e., a pebble starting with a lower IR_n than another will always have a lower IR_n than the other if they travel the same distance), then we can assume that each percentile represents a population that evolves downstream, and the linear fits represent sections of an
290 asymptotic trend that occurs over much longer distances, with a gradient decreasing rapidly as IR_n approaches the asymptote (Figure 5).

As rounding is driven by abrasion, we propose a rounding model that mirrors 'Sternberg's law' of abrasion which predicts that a pebble's size or mass will decay exponentially downstream under the effect of abrasion (Sternberg, 1875). This model is consistent with previous studies that have shown that there is a nonlinear relationship between transport distance and peb-
295 ble roundness (Wentworth, 1923; Miller et al., 2014). We begin by assuming that this nonlinear relationship extends to the relationship between IR_n and transport distance, and that the maximum IR_{max} value that will be asymptotically approached is unity. In other words, a pebble will eventually, given enough transport distance, become perfectly rounded. Based on these assumptions, we propose the following equation for the evolution of IR_n downstream:

$$IR_n = IR_{max} - ke^{-\lambda d} \tag{5}$$

300 where IR_{max} is the maximum roundness value that the pebble can achieve, which is theoretically 1, d is the transport distance, k is a prefactor value that controls the initial roundness of the pebble, and λ is a coefficient that defines the rate at which the pebbles round as a function of transport distance.

The advantage of this equation is that the coefficients λ and k can be obtained through linear regression of field data. The equation can be rearranged as follows:

305 $\ln(IR_{max} - IR_n) = \ln(ke^{-\lambda d})$ \hfill (6)
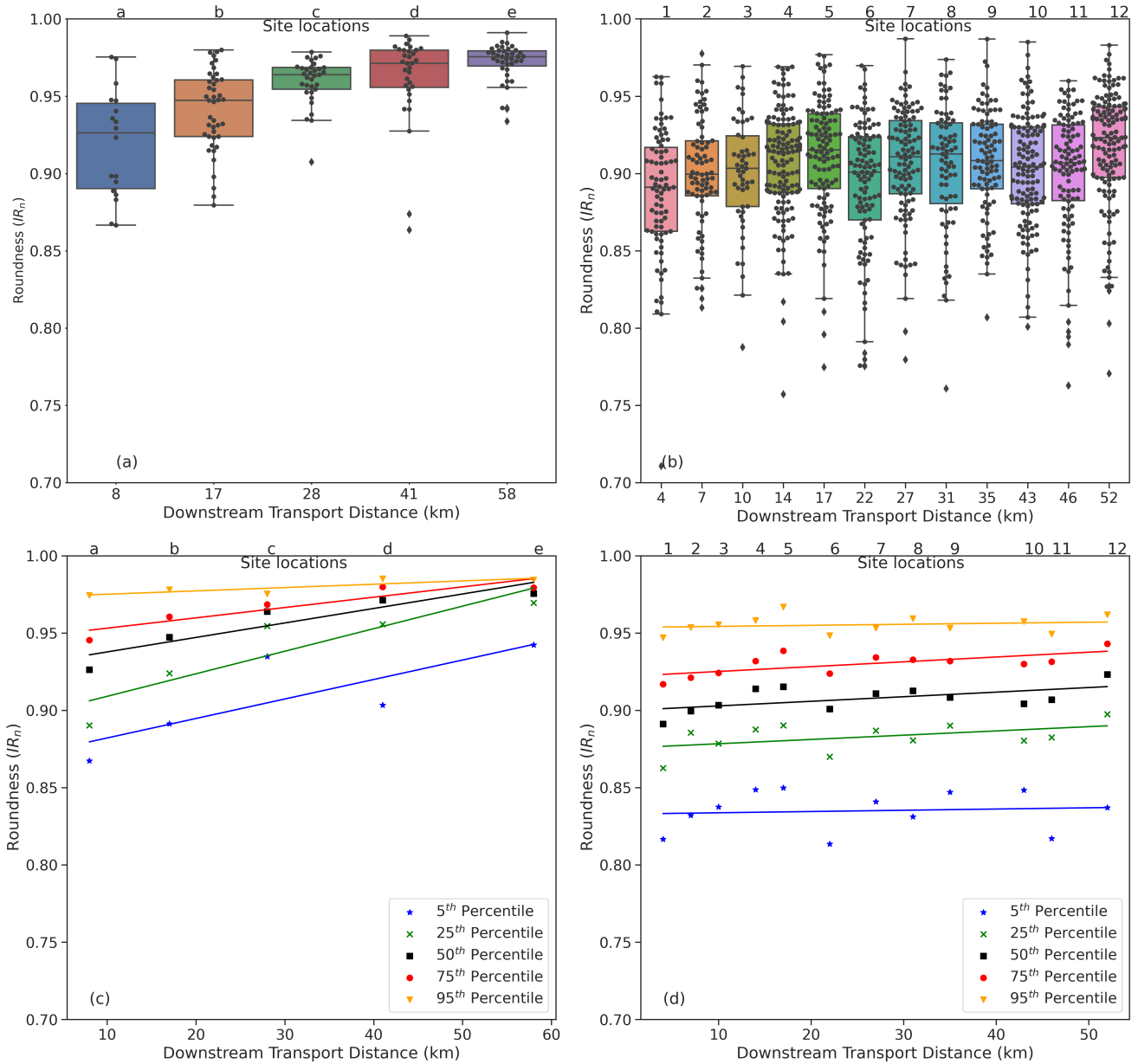
Figure 4. Box plots of the raw data showing the range of roundness values at each location for (**a**) granite pebbles and (**b**) quartzite pebbles. The bottom row shows linear fit to the downstream percentiles (5th, 25th, 50th, 75th and 95th) of (**c**) granite pebbles from Rapti and (**d**) quartzite pebbles from Banganga River. Note that the axes of the top figure is categorical such that the box plots are uniformly spaced and are not positioned by downstream distance.
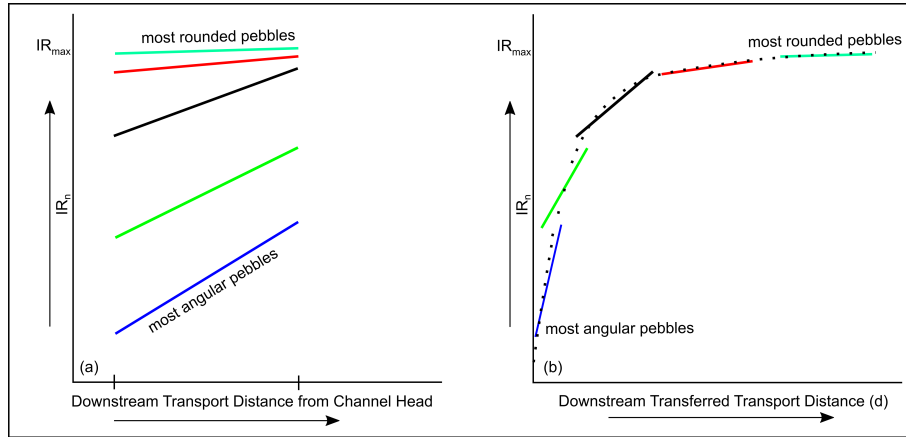
Figure 5. Schematic diagram showing our conceptual roundness model, including the idea that linear fits to each percentile data over a distance of 50 km represent the evolution of roundness for pebble populations starting their journey with different roundness values, and therefore represent various segments of the complete asymptotic roundness curve, with slope decreasing rapidly as IR_n approaches 1 (**a**). Reconstructing the complete roundness curve can be achieved by shifting each percentile data by an increasingly greater distance with increasing percentile (and therefore roundness) (**b**). See text (Sect. 3.2) for description of the approach developed to determine the best fit shifting distances.

As $IR_{max} = 1$, the equation becomes:

$$\ln(1 - IR_n) = \ln(k) + \ln(e^{-\lambda d}) \tag{7}$$

$$\ln(1 - IR_n) = \ln(k) - \lambda d \tag{8}$$

In a plot of $ln(1 - IR_n) = f(d)$, the slope of the linear regression is $-\lambda$ and the intercept $ln(k)$. In Sect. 3.2, we describe
310 how we process our data to derive the theoretical rounding curves and coefficients for our granite and quartzite pebbles.

3.2 Derivation of Rounding Curves and Coefficients for our Granite and Quartzite Pebbles

As mentioned earlier, we propose that the distance ($\sim$50 km) we covered in the field to collect the pebble roundness data is not sufficient to generate the complete roundness curve. We also propose that each percentile represents a given population of pebbles starting its journey with a given roundness, and that each fit to the percentile data over 50 km represents a section
315 of the complete roundness curve (Figure 5). Segments corresponding to greater percentiles have higher roundness values and lower slopes (in particular for the granite), and would therefore correspond to parts of the curve closer to the asymptote, i.e., further to the right (greater transport distance) in Figure 5. The challenge is to determine the transport distance by which each percentile data has to be shifted to the right to reconstruct the complete roundness curve.

The model we propose predicts a linear relationship between transport distance (d) and $ln(1-IR_n)$. We calculate $ln(1-IR_n)$
320 for all our field data, and run a sequential analysis to estimate by how much each percentile data have to be shifted in terms of distance to produce the best linear fit of $ln(1 - IR_n) = f(d)$ for each lithology. We begin by plotting $ln(1 - IR_n) = f(d)$ for

the 5th percentile data for all field locations. We then add the $ln(1 - IR_n)$ values for the 25th, 50th, 75th and 95th percentile data with the transport distance shifted by varying amounts further downstream.

Table 1. The transferred distances for each percentile that gives the best fit using the down hill gradient for granite pebbles.

Rock type:		Granite
Location:		[a, b, c, d, e]
Field distance (km):		[8, 17, 28, 41, 58]
Percentile	Transferred distance (km)	New distances (km)
5th percentile	0	[8, 17, 28, 41, 58]
25th percentile	21	[29, 38, 49, 62, 79]
50th percentile	37	[45, 54, 65, 78, 95]
75th percentile	51	[59, 68, 79, 92, 109]
95th percentile	80	[88, 97, 108, 121, 138]

Table 2. The transferred distances for each percentile that gives the best fit using the down hill gradient for quartzite pebbles.

Rock type:		Quartzite
Location:		[1, 2, 3, 4, 5, 6, 7, 8, 9, 10, 11, 12]
Field distance (km):		[4, 7, 10, 14, 17, 22, 27, 31, 35, 43, 46, 52]
Percentile	Transferred distance (km)	New distances (km)
5th percentile	0	[4, 7, 10, 14, 17, 22, 27, 31, 35, 43, 46, 52]
25th percentile	144	[148, 151, 154, 158, 161, 166, 171, 175, 179, 187, 190, 196]
50th percentile	245	[249, 252, 255, 259, 262, 267, 272, 276, 280, 288, 291, 297]
75th percentile	363	[367, 370, 373, 377, 380, 385, 390, 394, 398, 406, 409, 415]
95th percentile	553	[557, 560, 563, 567, 570, 575, 580, 584, 588, 596, 599, 605]

We use an optimisation technique to find the best-fitting linear regression model for a set of data points. The data consists

325 of distance data $X5$, $X25$, $X50$, $X75$, and $X95$, and the associated $ln(1 - IR_n)$ data corresponding to each percentile (5th, 25th, 50th, 75th and 95th). The distance $X5$ corresponding to the 5th percentile is kept as the original values from the field. The primary objective of the approach is to determine the optimal distances ($X25$, $X50$, $X75$, $X95$) that yield the best linear fit by transferring the roundness data from the 25th, 50th, 75th and 95th percentiles further downstream, thereby increasing transport distance d. We consider the $R-squared$ values (with vertical residue) as the evaluation metric.

330 The optimisation process used is the downhill gradient method, implemented through the 'scipy.optimise.minimise' function using 'Nelder-Mead' method (Nelder and Mead, 1965). This method aims to minimise the negative of the $R-squared$ values, effectively maximising the $R-squared$. The process starts with initial parameter values and iteratively adjusts these parameters
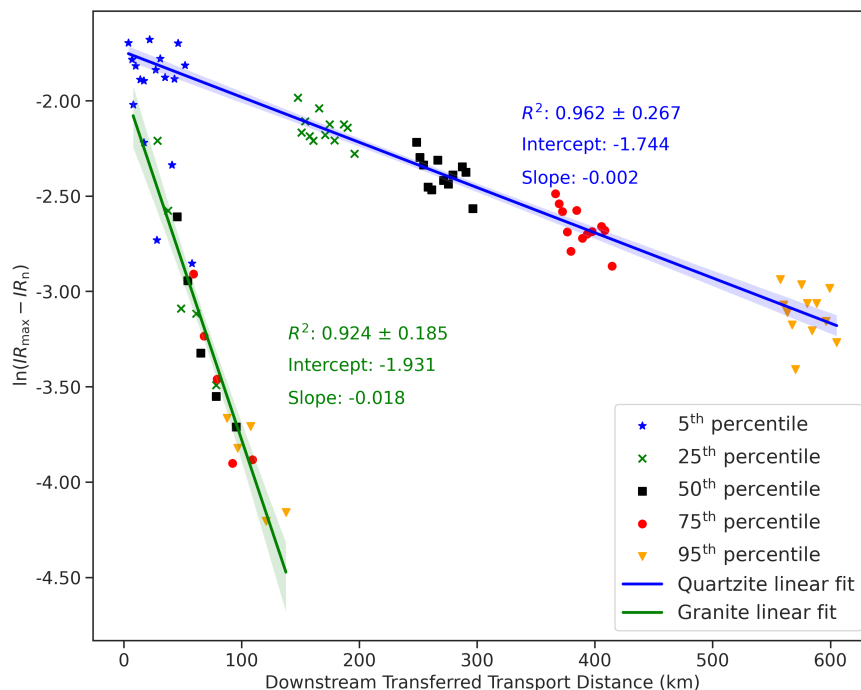
Figure 6. Plot of $\ln(IR_{max} - IR_n)$ against downstream transferred transport distance for granite pebbles and quartzite pebbles. Each marker and colour represents percentile roundness data. The blue and green lines represent the best linear fits of transferred percentile roundness data for quartzite and granite, respectively. Here, the x-axis is labelled 'Downstream Transferred Transport Distance' as each percentile data (25th, 50th, 75th and 95th) have been shifted / transferred a given distance downstream to obtain the best linear fit with $\ln(IR_{max} - IR_n)$. See text (Sect. 3.2) for description of the method of transferred distance.

to optimise the $R - squared$. The 'Nelder-Mead' method is selected as the optimisation algorithm due to its effectiveness in handling non-linear optimisation problems without requiring gradient information.

335   The function at first calculates the $R - squared$ value for the set of parameters ($ln(1 - IR_n)$ and d) and appends the $R - squared$, slope, and intercept values. It then proceeds to optimise the parameters using the 'minimise' function. Once the optimal parameters are determined, new distance values ($X25$, $X50$, $X75$, $X95$) are calculated using the optimised offsets. The new distances after the transformation of percentile is shown in Table 1 for granite pebbles and Table 2 for quartzite pebbles. The linear regression model is then fitted to the concatenated data ($X = X5, X25, X50, X75, X95$ and $Y = ln(1 - IR_n)$ from the 5th, 25th, 50th, 75th, and 95th percentiles, respectively) using the linear regression model. The value of the pre-factor k

340   derived from this optimisation technique is 0.145 and 0.174 for the granite and quartzite pebbles, respectively (Figure 6). The rounding coefficient λ is 0.018 and 0.002 for the granite and quartzite pebbles, respectively: the granite's λ is approximately seven times than that of quartzite. Based on these parameters, we can construct the theoretical roundness curve over longer distance for these two lithologies (Figure 7), which is described in Sect. 4.
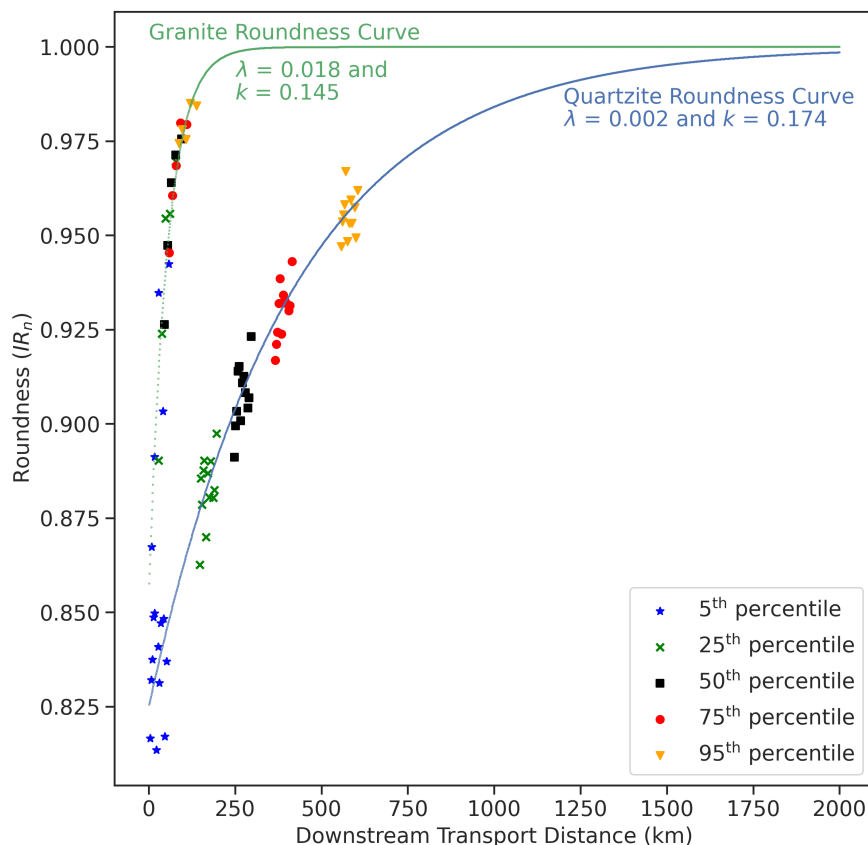
Figure 7. Theoretical roundness curve for granite (green) and quartzite (blue) derived from the optimisation method and regression of $ln(1 - IR_n) = f(d)$ field data. Each marker and colour represents field roundness data. The roundness coefficient of granite is around seven times that of quartzite.

4 Application of Roundness Model to Modern and Ancient Himalayan River Systems

4.1 Recycled Modern Pebbles

Today's large rivers of the Himalaya transport pebbles that can be broadly separated into two categories. The first are pebbles sourced from bedrock exposed in the catchment area, and the second are pebbles recycled from conglomerates by ancient river systems (Quick et al., 2019). Because the later category contains recycled clasts that may have gone through one or more cycles of transport, deposition, and re-entrainment, these pebbles will tend to have greater roundness than pebbles sourced from bedrock exposed in the catchment area.

Quick et al. (2019) studied pebbles in one of the antecedent Himalayan rivers (Karnali River) in the western part of Nepal. They observed more rounded pebbles relative to other Himalayan rivers (Kosi River in eastern Nepal). The difference was
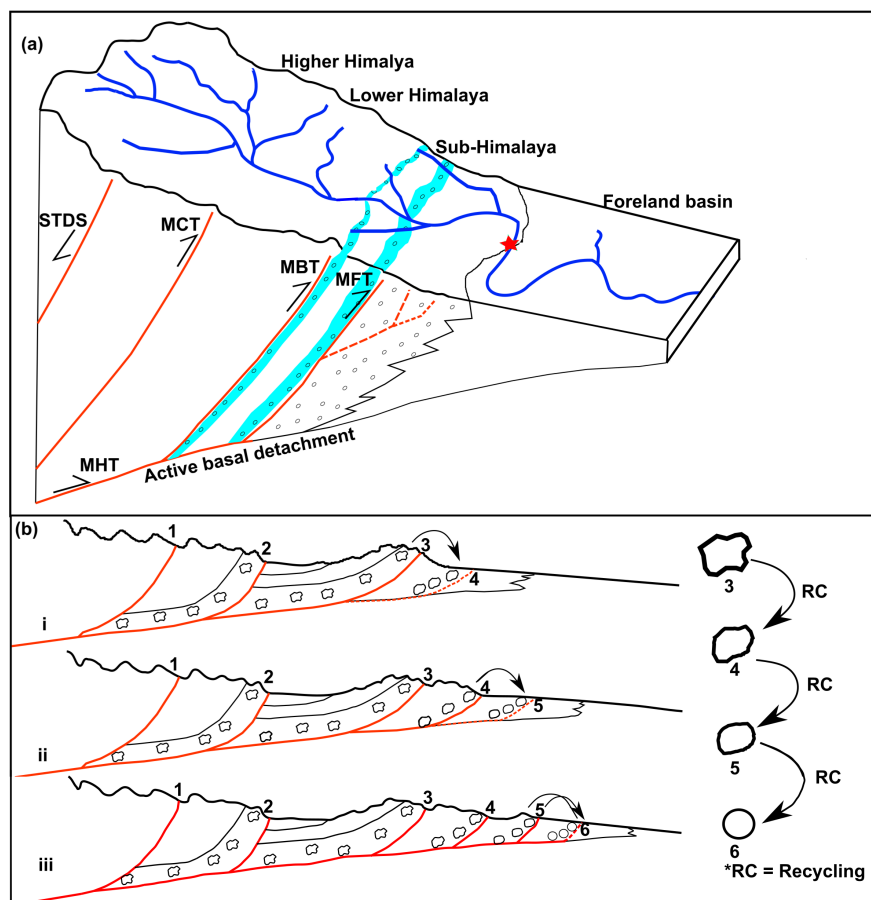
Figure 8. (**a**) Schematic diagram showing the major tectonic units of Himalaya, morphology and source for the recycled pebbles (Miocene-Pliocene conglomerate beds of Sub-Himalaya/Upper Siwaliks) along the Karnali River in western Nepal. Note: Sample site, marked by red star in the diagram, consists mixture of modern and recycled sediments. (**b**) Repeated cycles of deposition, uplift, erosion and transportation of sediments in foreland basin (since 16 Ma). Almost 90% of pebbles in sampling site are sourced from conglomerates of Siwaliks (Quick et al., 2019).

attributed to the presence of conglomerate in the Karnali that are not present in the Kosi catchment. The Sub-Himalaya (also
355 know as the Siwaliks) exposes these conglomerates and form the frontal hills north of the foreland basin of the Ganga Plains (See Figure 8). The provenance for the clasts in the Upper Siwaliks conglomerates are meta-sedimentary and metamorphic rocks of Higher and Lesser Himalaya (Zaheer et al., 2022). Consequently, the main channel of the Karnali River consist of first generation pebbles and boulder from the upstream part of the catchment mixed with recycled material from the frontal ranges.

The recycled pebbles from the Upper Siwaliks conglomerates may have experienced multiple cycles of deposition, tectonic
360 uplift and re-deposition as the proximal foreland basin is incorporated into the thrust wedge. The process how thrust wedges

consist accredited sediments from foreland basin and would have been sourced from and, then recycled back into the wedge is outlined by Sinclair (2011). In our study area, we do not know how many such cycles of uplift, erosion and re-deposition the conglomerate pebbles have experienced due to the ongoing shortening across the Himalaya. We can address these questions using our new rounding model. This is not without pitfalls, as the effect of weathering during a Upper Siwaliks conglomerates

365 time deposited as sediment can affect its resistance to abrasion once it is re-entrained. However, the difference in roundness among recycled and non-recycled pebbles can still be used to consider the paleo-transport distance of pebbles that are considered to have been recycled .

In this case, we have used field data from Quick et al. (2019). The Sub-Himalaya in this region consists thick (several tens of meters) Miocene-Pliocene conglomerate beds comprising clasts of quartzite, marble, schist, phyllite, dolomite and limestone.

370 These clasts from the Sub-Himalaya tributaries are eroded and mixed with the other modern sediment along the Karnali River. The Sample site is located in the Indo-Gangetic plain which consist of a full mixture of sediments from Higher to Lesser Himalaya and Sub-Himalaya (Sample site in Figure 8), where 95th percentile roundness is 0.995 and 5th percentile roundness is 0.908 for quartzite pebbles. The calculated maximum transport distance is based on the 95th percentile of roundness data of quartzite pebbles collected along the Karnali River (Figure 9).

375 We compare modern length of the Karnali River (from channel head to the sampling site) with the transport distance of pebbles calculated using our new model. This calculation is based on the assumption that the quartzite pebbles collected along the Karnali River behaves in a similar way as the quartzite pebbles used to generate the roundness curve in this study. The maximum transport distances for the quartzite pebbles calculated using the 95th roundness percentiles is 1472 km (Figure 9) at sampling site whereas the length of modern Karnali River from channel-head to sampling site is only 660 km (see Figure 2 and

380 Figure 8). The maximum transport distance for the pebbles at sampling site is greater than the length of modern Karnali River . This implies that a proportion of the pebbles in the modern river were recycled to a distance equivalent to ~ 800 km of transport and abrasion. Hence, it supports the interpretation by Quick et al. (2019) that recycled sediments from the conglomerates are likely to explain the difference between the modern length of river and the calculated transport distance based on the rounding of pebbles.

385 **4.2 Pebbles from the stratigraphic record**

A broader application of our method is to calculate the transport distance of ancient river deposits preserved in the stratigraphic record. The Kathmandu Valley in central Nepal is a perched sedimentary basin (Sakai et al., 2006) that has its headwaters south of the main Himalayan drainage divide. There has been some speculation that the location of the headwaters of this catchment were previously in the high Himalaya (Hagen, 1969). In order to test this, we chose to assess transport distances based on

390 rounding of pebbles in Quaternary fluvial deposits.

Samples were collected from a site exposed by incision of the Bagmati River (see Figure 2 and Figure 10) which is the main drainage of the Kathmandu Basin. The sampling site is a ~ 2.5 Ma old deposit (Yoshida and Igarashi, 1984) that consists of gravel beds underlain by basement rock and overlain by lacustrine deposits (see Figure 11). Quartzite and granite are the most dominant rock types among the clasts found in the conglomerates (marked by star in Figure 11) within the fluvial deposit. It
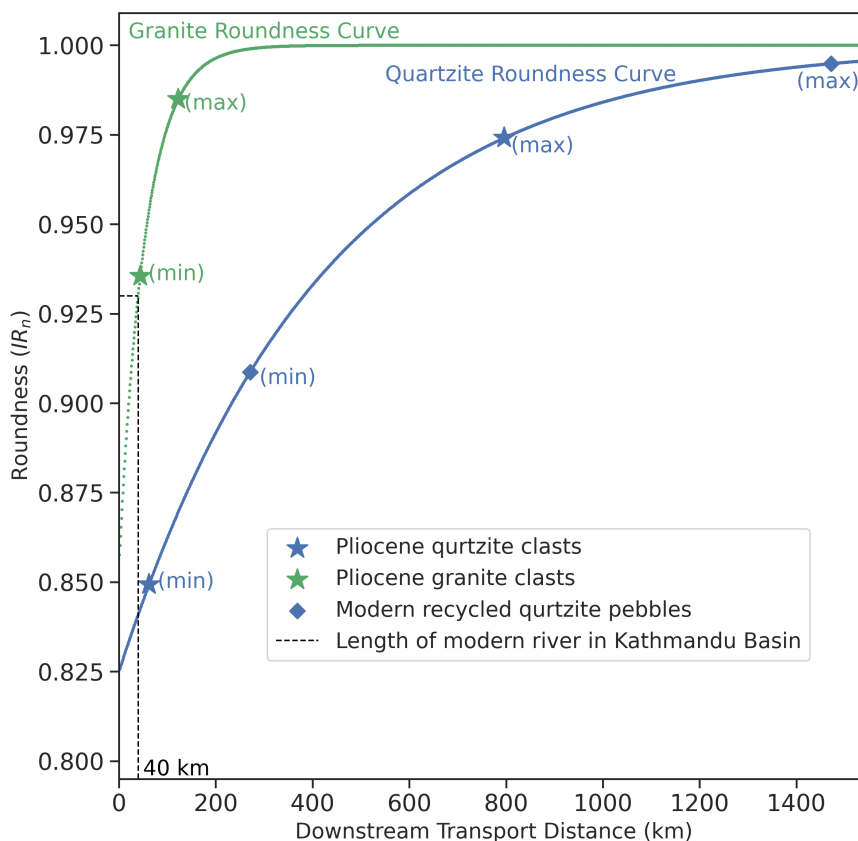
Figure 9. Application of model on Pliocene conglomerate clasts from the Kathmandu Basin and modern recycled pebbles from the Karnali River. The range of likely transport distances for the Pliocene clasts is calculated using 5th percentile and 95th percentile. The minimum calculated transport distance (44 km for granite clasts and 62 km for quartzite clasts) is greater than the length (40 km) of modern river (Bagmati River) within the Kathmandu Basin. Similarly, the range of likely transport distances for modern recycled pebbles calculated using 5th percentile and 95th percentile is 270-1472 km.

395   is important to note that the granite clasts are absent in the alluvial fan deposits. We measured the roundness of both quartzite and granite pebbles to mirror our measurements in modern channels. Based on the 5th and the 95th percentiles of measured IR_n values, we calculate the range of probable transport distances travelled by the pebbles using the roundness curve shown in Figure 7. The minimum transport distance (using 5th percentile) is 44 km for granite clast and 62 km for quartzite clast (Figure 9). The maximum transport distance (using 95th percentile) is 123 km for granite clasts and 795 km for quartzite clasts

400   (Figure 9). The measured length of the modern river from channel head (Bagmati River) inside the Kathmandu Basin is only 40 km (Figure 10). The minimum transport distance calculated from the pebble roundness is higher than the length of modern channel inside the Kathmandu Basin.
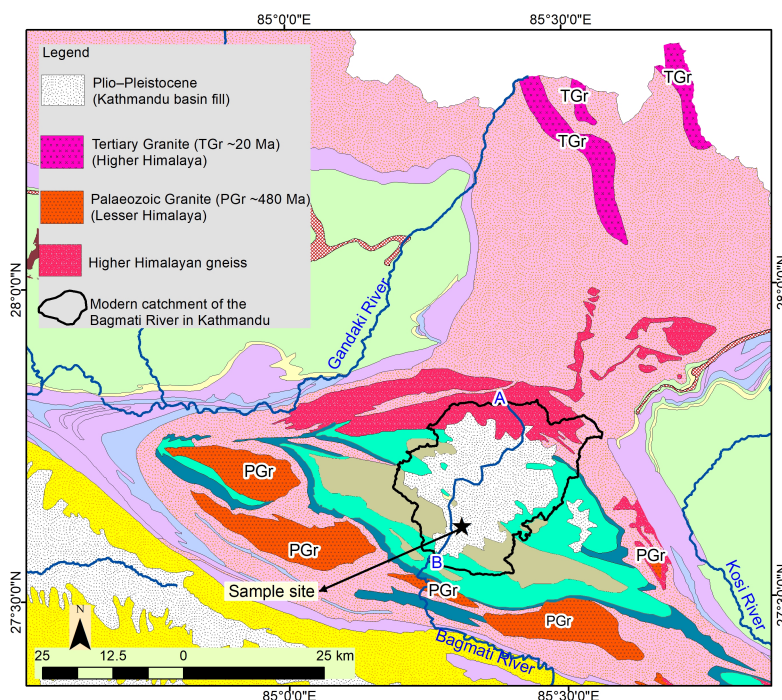
Figure 10. Regional geological map showing the occurrence of 2 possible sources (Tertiary Granite (TGr) in Higher Himalaya and Paleozoic Granite (PGr) in Lesser Himalaya) for the granite pebbles found at the base of the Kathmandu Basin. Note: both granites (TGr and PGr) are outside of the catchment area of the modern Bagmati River in Kathmandu. Map source: Geological map of central Nepal by Department of Mines and Geology in Nepal (Department of Mines and Geology, 2011).

In addition, when we investigate the regional geological map (Figure 10) around the Kathmandu Basin in central Nepal, we do not find any granitic intrusion within the catchment area of the modern Bagmati River inside the Kathmandu Basin. However, there are Paleozoic granites just outside the Kathmandu Basin to the south, and Tertiary granites are located outside the basin to the north (refer to the regional geological map of central Nepal in Figure 10). Consequently, the greater paleo-transport distance of Pliocene granite clasts and the absence of granite source rock in the modern catchment area of the Bagmati River supports the previously hypothesised extensive drainage network (Hagen, 1969) through the present Kathmandu Basin."

5 Discussion

A number of researchers have previously evaluated the roundness of pebbles transported by rivers. For example, Wentworth (1922), Mills (1979), and Miller et al. (2014) discussed the downstream evolution of pebble along the river system. Wentworth (1923), Mills (1979), Miller et al. (2014) and Gale (2021) suggested a non-linear relationship between roundness and transport distance; here, we have expanded on this by empirically relating roundness to transport distance in the setting of the Himalayan rivers. The model we propose is not limited to the single median or average value for a particular location as done by Wentworth
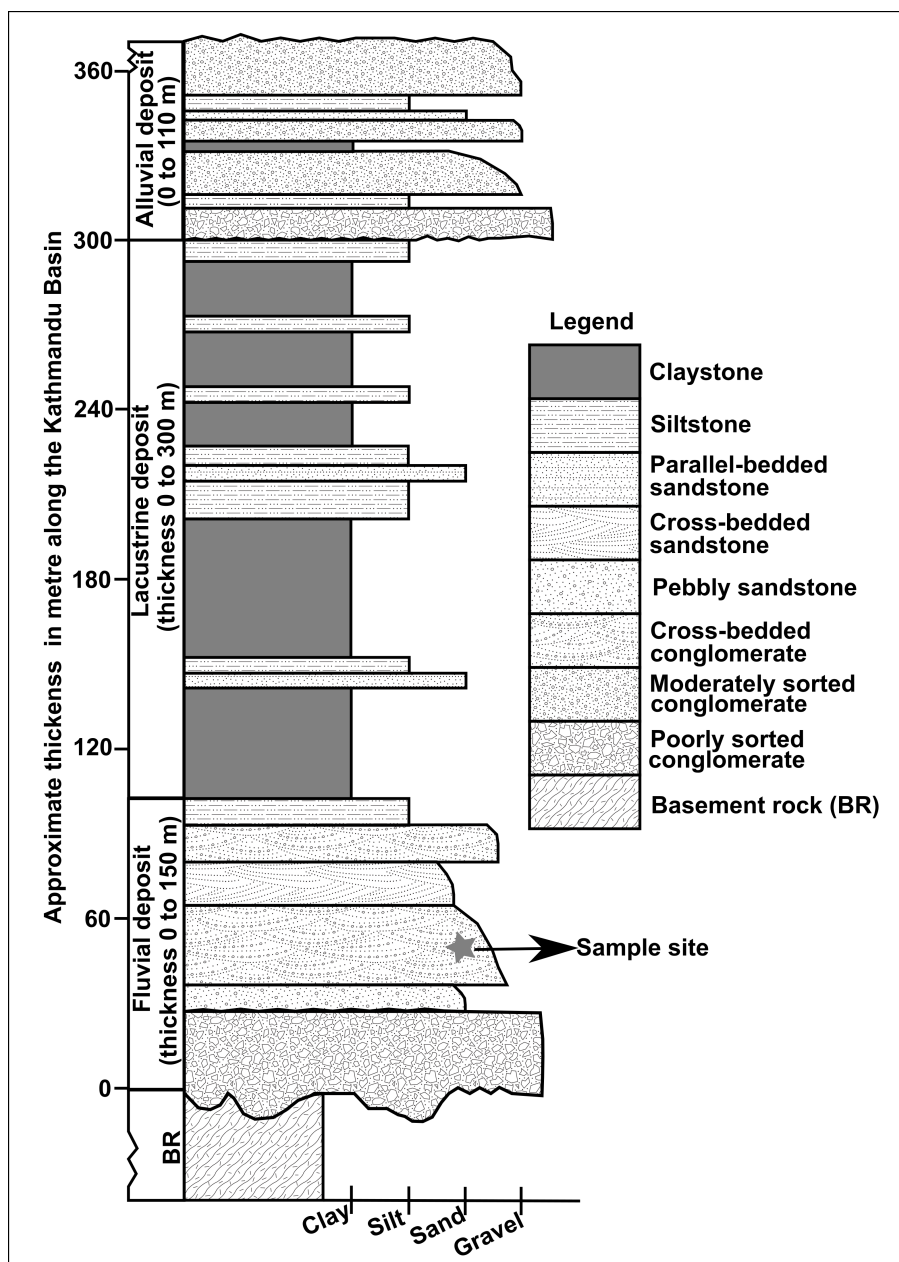
Figure 11. A representative sedimentary succession observed in various parts of the Kathmandu Basin. Pliocene mass-flow type conglomerates and fluvial gravel-sand deposits unconformably overlie the Paleozoic basement rock. Above these deposits, Pliocene-Pleistocene lacustrine clay-silt sediments mostly fill the central part of the basin. Notably, in the southern part of the basin, high-level terraces have formed as a result of alluvial fans of Pliocene-Pleistocene age from Mahabhart Range.

415   (1923), Quick et al. (2019) and others. The reason why we consider the percentile distribution is that from field observations we observe that pebbles of identical lithologies, similar size, and the same transport distance downstream, may exhibit very different roundness values (see Figure 12, similar to the observation made by Gale (2021). By combining different percentile groups of roundness, we are able to construct rounding curves, which are consistent with a non-linear relationship between rounding and transport distance proposed by previous studies. With this model, the rounding curves for pebbles depend on the

420   coefficient of roundness (λ) and prefactor (k).

    Variations in the coefficient of roundness (λ) are observed among different rock types. The λ for quartzite and granite pebbles from the Himalayan river were calculated using field data, and it was found that granite is significantly more susceptible to rounding than quartzite. This result is consistent with previous studies on the control of lithology on abrasion and roundness (Kuenen, 1956; Sneed and Folk, 1958; Kodama, 1994; Lindsey et al., 2005).

425   The prefactor (k) is another parameter in the model that indicates the predicted starting roundness of pebbles. However, the roundness of pebbles, even of the same rock type, varies significantly at a particular location. For example, in Figure 12, the roundness value ranges from 0.867 to 0.975 for granite pebbles from the most upstream location 'a' along the Rapti River in our study area, as shown in Figure 2 (d). Although the pebble with a roundness value of 0.975 (IR_n) in the top left corner of Figure 12 had travelled only 8 km from the channel head, it possessed a roundness value equivalent to a downstream transport distance

430   of 50 km (see Figure 4a). Clearly, clasts fed into a river, even from areas of the same rock type with similar sediment production processes (weathering, erosion, and transportation), will not have identical roundness. The different mechanism of sediment production, such as bank erosion, mass wasting, landslide, hill-slope erosion, duration of exposure to weathering conditions, and boundary conditions during the flow may impact the roundness of pebbles. Both experimental observations and modelling results indicate that sediment undergoes intermittent motion, resembling a succession of periods involving "flight" and periods

435   of rest, as described by (Lajeunesse et al., 2010). Additionally, we hypothesise that some pebbles that travel through cavities and pools along the upper reaches of the river channel possess higher degrees of roundness. Hence, each pebble has a different rounding history based on the initial roundness and transport mechanism.

    We emphasise that the prefactor (k) and coefficient of roundness (λ) derived from our study are specific to quartzite and granite pebbles found in the two small catchments of the Himalayan river. The quartzite pebbles are sourced from a massive

440   bed of mono-mineralic (quartz) quartzite while the granite pebbles are rich in feldspar and mica minerals. Therefore, the values obtained in this study should not be used as universal values for all granite and quartzite pebbles. However, we do believe that non-linear relationship between roundness and transport distance applies to all pebbles where downstream rounding is controlled by the abrasion process. It is important to note that pebbles sourced from thinly bedded (shale) or highly foliated (slate, schist) bedrock may have a different story when it comes to downstream rounding, where the shape and size in downstream

445   changes are due to processes other than abrasion (e.g. fracturing). However, it is noteworthy that the parameter (IR_n) used in this model to represent the roundness is independent of sphericity. Thus, we acknowledge that the roundness coefficient and prefactor may vary in other catchments based on factors such as hardness, lithology, climate, tectonics, and sediment production process. Nonetheless, the concept of the model will still be valid. Therefore, we encourage the application of this model in other parts of the world to generate the prefactor (k) and coefficient of roundness (λ) in different geomorphic settings.

450   Downstream fining and rounding of pebbles are influenced by the concept of size-dependent roundness/shape. In this study, pebbles ranging from granules to cobbles were collected from the river's channel deposit. We did not categorise the sediment based on grain size, as we believe that Quick (2021) showed no correlation between downstream fining and rounding of grains. Whether our model is applicable to downstream rounding of fine particles, such as sand and silt is uncertain as it depends on the nature of the abrasion processes and hence grain interactions during transport; naturally, the more sediment is transported

455   in suspension, the less it will experience abrasion.
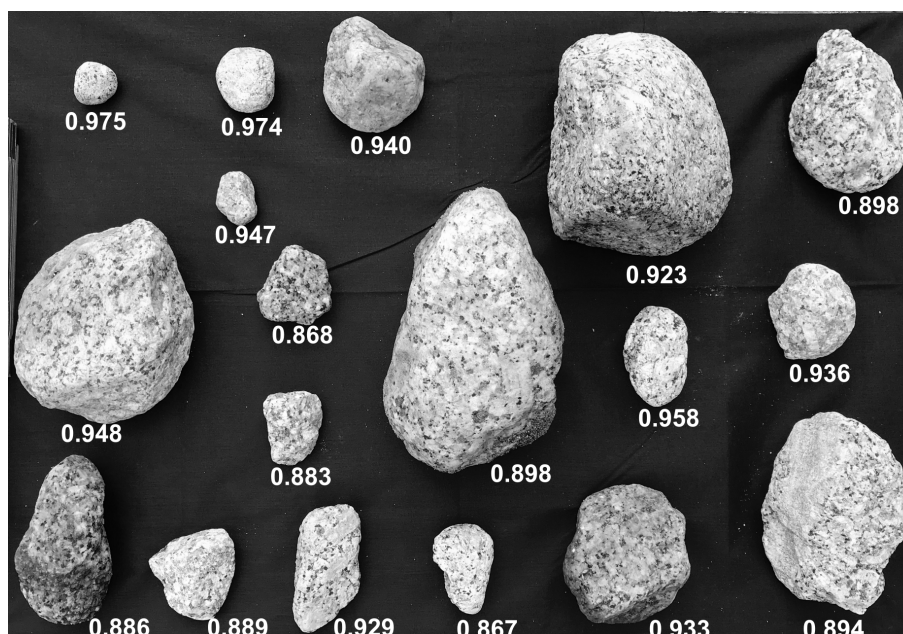
Figure 12. Photograph showing the roundness value for the location 'a' ($\sim$ 8 km downstream from channel head) in Figure 2 (d). Note that the roundness value for this location ranges from 0.867 to 0.975. Though the pebble with 0.98 roundness had travelled only 8 km transport distance from the channel head, its roundness is equivalent to the pebbles which have travelled 50 km transport distance and hence this implies that the roundness of pebbles at any location depends on the initial roundness of pebbles/rock fragment before being transported along the rivers.

We present the applicability of new roundness model to the ancient and modern sediments. Using the roundness curves generated from this study, we estimated transport distance for the pebbles. Nonetheless, uncertainties associated with the estimated transport distances are significant. We use roundness data measured by Quick (2021) for the modern pebbles along the Karnali River. The roundness for the Pliocene clasts are measured during this study. The estimated transport distance

460   assumes that the initial roundness of pebbles/rock fragment along the Karnali and Pliocene Bagmati River had the similar initial roundness as used in this model. Additionally, the Karnali River and the Pliocene equivalent of the Bagmati River are trans-Himalayan rivers, while the roundness coefficient (λ) and prefactor (k) used in this study are derived from a smaller Lesser Himalayan catchments. Consequently, the estimated transport distance assumes similar abrasion processes/rate in both trans-

Himalayan rivers and smaller rivers with limited catchment area. Clearly, the impact of glacial sources for trans-Himalayan
rivers are likely to provide different roundness values on entering the fluvial system.

Overall, we present the roundness curves based on field-measured data, and we are confident that other sediments also
exhibit similar transport histories in fluvial environment. The parameters (λ) and prefactor (k) encompass information related
to various factors, and we believe future research will isolate the specific impacts of these factors. Most notably, this study
establishes the groundwork for quantifying transport distances based on sediment roundness.

6 Conclusions

– A methodology that measures the pebble silhouette using a colour threshold to differentiate the background and pebble
area in the 2D photographs has been generated that enables automated extraction of pebble roundness and hence ensures
the replication of measurements.

– A normalized Isoperimetric ratio (IR_n) of pebble outline is used to parameterise the roundness (/angularity) of modern
river pebbles and ancient clasts in the stratigraphic record. This parameter is easy to measure and independent from the
sphericity.

– The method has been applied to pebbles from two rivers that drain the sub-Himalaya and frontal regions of the Himalaya
and which have either granite or quartzite exposed in their upper headwaters.

– Consistent with previous studies, we have shown a nonlinear relationship between transport distance and pebble round-
ness. We propose a new model that mirrors 'Sternberg's law' of abrasion and using the field data we generate roundness
curves for two lithologies (quartzite and granite) and these curves give the estimate of transport distance beyond our
study reaches.

– Using our new model, we demonstrate that rates of rounding decrease with distance downstream to form a negative
exponential. The degree of rounding against downstream distance varies as a function of lithology, with granites rounding
faster than quartzites.

– Using the calibrated model of rounding rates, we give support to previous theories that indicate that the recycling of
clasts from conglomerates impacts the degree of rounding of some trans-Himalayan rivers as they exit the mountain
front.

– Conglomerates from Pliocene fluvial deposits in the Kathmandu Basin comprise relatively more rounded quartzite peb-
bles that suggest paleo-transport distances that are greater than the current length of the Bagmati River in the basin. We
propose that this supports previous suggestions that the paleo-Bagmati River was significantly larger than the present-day
equivalent, and that the catchment has reduced in size.

Code and data availability. Data will be made available via the Edinburgh DataShare once the manuscript gets accepted by the editorial board.

495 *Author contributions.* MA and PP developed the concept. PP conducted the fieldwork and data analysis. MA, HDS, SMM, and MN provided motivation for the study and contributed to the development of the ideas. PP wrote the paper. All authors contributed to revising the text and figures.

Competing interests. At least one of the (co-)authors is a member of the editorial board of Earth Surface Dynamics.

Acknowledgements. We express our gratitude to Subash Acharya, Puspa Raj Dahal, Mahesh Raut, Ravi Nepal, and Khim Bahadur Khadka
500 for their invaluable support during the fieldwork. Additionally, we extend our thanks to the Tomorrow's Cities' Kathmandu Hub for generously providing financial support for this research. We also acknowledge that this study forms a part of a Ph.D. program funded by the School of GeoSciences-University of Edinburgh (UKRI GCRF Tomorrow's Cities Hub, Grant number: NE/S009000/1).

References

Abbott, P. L. and Peterson, G. L.: Effects of abrasion durability on conglomerate clast populations; examples from Cretaceous and Eocene
505   conglomerates of the San Diego area, California, Journal of sedimentary petrology, 48, 31–42, https://doi.org/10.1306/212F73EC-2B24-
    11D7-8648000102C1865D, 1978.

Attal, M. and Lave, J.: Changes of bedload characteristics along the Marsyandi River (central Nepal): Implications for understanding hillslope
    sediment supply, sediment load evolution along fluvial networks, and denudation in active orogenic belts, vol. 398, Geological Society of
    America, https://doi.org/10.1130/2006.2398(09), 2006.

510 Attal, M. and Lave, J.: Pebble abrasion during fluvial transport: Experimental results and implications for the evolution of the sediment load
    along rivers, Journal of Geophysical Research, 114, https://doi.org/10.1029/2009jf001328, 2009.

Attal, M., Lave, J., and Masson, J.-P.: New Facility to Study River Abrasion Processes, Journal of Hydraulic Engineering, 132, 624–628,
    https://doi.org/10.1061/(ASCE)0733-9429(2006)132:6(624), 2006.

Barrett, P. J.: The shape of rock particles, a critical review, Sedimentology, 27, 291–303, https://doi.org/10.1111/j.1365-3091.1980.tb01179.x,
515   1980.

Blott, S. J. and Pye, K.: Particle shape: a review and new methods of characterization and classification, Sedimentology, 55, 31–63,
    https://doi.org/https://doi.org/10.1111/j.1365-3091.2007.00892.x, 2008.

Brewer, P. A. and Lewin, J.: In-Transport Modification of Alluvial Sediment: Field Evidence and Laboratory Experiments, pp. 23–35,
    https://doi.org/10.1002/9781444303995.ch3, 1993.

520 Cassel, M., Piégay, H., Lavé, J., Vaudor, L., Hadmoko Sri, D., Wibiwo Budi, S., and Lavigne, F.: Evaluating a 2D image-based computer-
    ized approach for measuring riverine pebble roundness, Geomorphology, 311, 143–157, https://doi.org/10.1016/j.geomorph.2018.03.020,
    2018.

Cottet, M.: Mesure et structures spatiales et temporelles de l'é mousse des galets dans le réseau hydrographique du Bez (On the measurement,
    the spatial and temporal distribution of pebble roundness in the hydrographic network of the Bez), p. 72, master's thesis, 2006.

525 Cox, E. P.: A Method of Assigning Numerical and Percentage Values to the Degree of Roundness of Sand Grains, Journal of paleontology,
    1, 179–183, 1927.

Cruz-Matías, I., Ayala, D., Hiller, D., Gutsch, S., Zacharias, M., Estradé, S., and Peiró, F.: Sphericity and roundness computation for particles
    using the extreme vertices model, Journal of Computational Science, 30, 28–40, https://doi.org/10.1016/j.jocs.2018.11.005, 2019.

Department of Mines and Geology: Geological map of central Nepal, Geological Mapping section, DMG, 2011.

530 Dhital, M. R.: Geology of the Nepal Himalaya: Regional Perspective of the Classic Collided Orogen, Cham: Springer International Publishing
    AG, Cham, 2015 edn., https://doi.org/10.1007/978-3-319-02496-7, 2015.

Diepenbroek, M., BartholomÄ, A., and Ibbeken, H.: How round is round? A new approach to the topic 'roundness'by Fourier grain shape
    analysis, Sedimentology, 39, 411–422, https://doi.org/10.1111/j.1365-3091.1992.tb02125.x, 1992.

Dobkins, J. and Folk, R. L.: Shape development on Tahiti-Nui, Journal of sedimentary petrology, 40, 1167–1203,
535   https://doi.org/10.1306/74D72162-2B21-11D7-8648000102C1865D, 1970.

Domokos, G., Sipos, A., Szabó, T., and Várkonyi, P.: Pebbles, Shapes, and Equilibria, Mathematical Geosciences, 42, 29–47,
    https://doi.org/10.1007/s11004-009-9250-4, 2009.

Domokos, G., Jerolmack, D. J., Sipos, A. A., and Torok, A.: How river rocks round: resolving the shape-size paradox, PLoS One, 9, e88 657,
    https://doi.org/10.1371/journal.pone.0088657, 2014.

540   Durian, D. J., Bideaud, H., Duringer, P., Schroder, A., Thalmann, F., and Marques, C. M.: What is in a pebble shape?, Phys Rev Lett, 97,
       028 001, https://doi.org/10.1103/PhysRevLett.97.028001, 2006.

Fehér, E., Havasi-Tóth, B., and Ludmány, B.: A new workflow for the automated measurement of shape descriptors of rocks, Earth Surf.
       Dynam. Discuss., 2020, 1–15, https://doi.org/10.5194/esurf-2020-23, 2020.

Gale, S. J.: The Shape of Fluvial Gravels: Insights from Fiji's Sabeto River, Geosciences, 11, 161,
545   https://doi.org/10.3390/geosciences11040161, 2021.

Hagen, T.: Report on the Geological Survey of Nepal, Denkschr. Schweiz. Naturf. Ges., 81, 185, 1969.

Howard, J. L.: An evaluation of shape indices as palaeoenvironmental indicators using quartzite and metavolcanic clasts in Upper Cre-
       taceous to Palaeogene beach, river and submarine fan conglomerates, Sedimentology, 39, 471–486, https://doi.org/10.1111/j.1365-
       3091.1992.tb02128.x, 1992.

550   Japan Aerospace Exploration Agency: ALOS World 3D 30 meter DEM. V3.2, https://doi.org/10.5069/G94M92HB, accessed on 2023-02-02,
       2021.

Jerolmack, D. J.: Pebbles on Mars, Science (American Association for the Advancement of Science), 340, 1055–1056,
       https://doi.org/10.1126/science.1239343, 2013.

Kodama, Y.: Experimental study of abrasion and its role in producing downstream fining in gravel-bed rivers, Journal of Sedimentary
555   Research, 64, 76–85, https://doi.org/10.2110/jsr.64.76, 1994.

Kuenen, P. H.: Experimental Abrasion of Pebbles: 2. Rolling by Current, The Journal of Geology, 64, 336–368, http://www.jstor.org/stable/
       30056065, 1956.

Lajeunesse, E., Malverti, L., and Charru, F.: Bed load transport in turbulent flow at the grain scale: Experiments and modeling, Journal of
       Geophysical Research: Earth Surface, 115, https://doi.org/10.1029/2009JF001628, 2010.

560   Lindsey, D. A., Langer, W. H., and Knepper, D. H.: Stratigraphy, lithology, and sedimentary features of Quaternary alluvial de-
       posits of the South Platte River and some of its tributaries east of the Front Range, Colorado, USGS-Technical report, 1705,
       https://doi.org/10.3133/pp1705, 2005.

Lindsey, D. A., Langer, W. H., and Van Gosen, B. S.: Using pebble lithology and roundness to interpret gravel provenance in piedmont fluvial
       systems of the Rocky Mountains, USA, Sedimentary Geology, 199, 223–232, https://doi.org/10.1016/j.sedgeo.2007.02.006, 2007.

565   Litty, C. and Schlunegger, F.: Controls on Pebbles' Size and Shape in Streams of the Swiss Alps, The Journal of Geology, 125, 101–112,
       https://doi.org/10.1086/689183, 2017.

McPherson, H. J.: Downstream Changes in Sediment Character in a High Energy Mountain Stream Channel, Arctic and Alpine Research, 3,
       65–79, https://doi.org/10.2307/1550383, 1971.

Miller, K. L., Szabó, T., Jerolmack, D. J., and Domokos, G.: Quantifying the significance of abrasion and selective transport for downstream
570   fluvial grain size evolution, Journal of Geophysical Research: Earth Surface, 119, 2412–2429, https://doi.org/10.1002/2014jf003156,
       2014.

Mills, H. H.: Downstream rounding of pebbles; a quantitative review, Journal of Sedimentary Research, 49, 295–302,
       https://doi.org/10.1306/212F7720-2B24-11D7-8648000102C1865D, 1979.

Mudd, S., Clubb, F., Grieve, S., Milodowski, D., Gailleton, B., Hurst, M., Valters, D., Wickert, A., and Hutton, E.: LSDtopotools/LSDTopo-
575   Tools2: LSDTopoTools2 v0.7, https://doi.org/10.5281/zenodo.7076014, 2022.

Nelder, J. A. and Mead, R.: A Simplex Method for Function Minimization, The Computer Journal, 7, 308–313,
       https://doi.org/10.1093/comjnl/7.4.308, 1965.

Novák-Szabó, T., Sipos, A. , Shaw, S., Bertoni, D., Pozzebon, A., Grottoli, E., Sarti, G., Ciavola, P., Domokos, G., and Jerolmack, D. J.: Universal characteristics of particle shape evolution by bed-load chipping, Science Advances, 4, eaao4946, https://doi.org/10.1126/sciadv.aao4946, 2018.

Purinton, B. and Bookhagen, B.: Introducing PebbleCounts: a grain-sizing tool for photo surveys of dynamic gravel-bed rivers, Earth Surf. Dynam., 7, 859–877, https://doi.org/10.5194/esurf-7-859-2019, eSurf, 2019.

Quick, L.: The Sediment Dynamics of the Himalayan Foreland Basin from the Neogene to Present Times, p. 315, Ph.D. thesis at University of Edinburgh-UK, 2021.

Quick, L., Sinclair, H. D., Attal, M., and Singh, V.: Conglomerate recycling in the Himalayan foreland basin: Implications for grain size and provenance, GSA Bulletin, 132, 1639–1656, https://doi.org/10.1130/B35334.1, 2019.

Roussillon, T., Piegay, H., Sivignon, I., Tougne, L., and Lavigne, F.: Automatic computation of pebble roundness using digital imagery and discrete geometry, Computers Geosciences, 35, 1992–2000, https://doi.org/10.1016/j.cageo.2009.01.013, 2009.

Russell, T.: Use of clast shape in determining the sedimentary history of the late devonian keepit conglomerate, Australia, Sedimentary Geology, 25, 277–290, https://doi.org/10.1016/0037-0738(80)90065-2, 1980.

Sakai, H.: Geology of the Tansen Group of the Lesser Himalaya in Nepal, Memoirs of the Faculty of Science, Kyūsyū University. Series D, Geology, 25, 27–74, https://doi.org/10.5109/1546083, 1983.

Sakai, H., Sakai, H., Yahagi, W., Fujii, R., Hayashi, T., and Upreti, B. N.: Pleistocene rapid uplift of the Himalayan frontal ranges recorded in the Kathmandu and Siwalik basins, Palaeogeography, Palaeoclimatology, Palaeoecology, 241, 16–27, https://doi.org/10.1016/j.palaeo.2006.06.017, 2006.

Schneider, C. A., Rasband, W. S., and Eliceiri, K. W.: NIH Image to ImageJ: 25 years of image analysis, Nature Methods, 9, 671–675, https://doi.org/10.1038/nmeth.2089, 2012.

Sinclair, H. D.: Thrust Wedge/Foreland Basin Systems, Tectonics of sedimentary basins: Recent advances, pp. 522–537, https://doi.org/10.1002/9781444347166.ch26, wiley Online Books, 2011.

Sneed, E. D. and Folk, R. L.: Pebbles in the Lower Colorado River, Texas a Study in Particle Morphogenesis, The Journal of geology, 66, 114–150, https://doi.org/10.1086/626490, 1958.

Sternberg, H.: Untersuchungen uber Langen- und Querprofilgeschiebefuhrender Flusse, Zeitshrift fur Bauwesen, 25, 483–506, 1875.

Szabo, T., Domokos, G., Grotzinger, J. P., and Jerolmack, D. J.: Reconstructing the transport history of pebbles on Mars, Nat Commun, 6, 8366, https://doi.org/10.1038/ncomms9366, 2015.

Tunwal, M., Mulchrone, K. F., and Meere, P. A.: Image based Particle Shape Analysis Toolbox (IPSAT), Computers Geosciences, 135, https://doi.org/10.1016/j.cageo.2019.104391, 2020.

Vanbrabant, C., Regnauld, H., and Duchesne, F.: La détermination pratique des intervalles de confiance des comptages de cailloux et des mesures d'émoussé. Comparaison des mesures d'émoussé de Cailleux et de Krumbein/Determination of confidence limits characterizing gravel pétrographie counts and roundness values. Comparison of roundness values by the Cailleux and the Krumbein methods, Géomorphologie : relief, processus, environnement, pp. 195–214, https://doi.org/10.3406/morfo.1998.955, 1998.

Villarino, M. B.: Ramanujan's Perimeter of an Ellipse, arXiv preprint math/0506384, https://arxiv.org/pdf/math/0506384.pdf, 2005.

Wadell, H.: Volume, Shape, and Roundness of Quartz Particles, The Journal of geology, 43, 250–280, https://doi.org/10.1086/624298, 1935.

Wentworth, C. K.: A Laboratory and Field Study of Cobble Abrasion, The Journal of geology, 27, 507–521, https://doi.org/10.1086/622676, 1919.

Wentworth, C. K.: A field study of the shapes of river pebbles, US Geological Survey Bulletin, 730, 103–114, 1922.

Wentworth, C. K.: A method of measuring and plotting the shapes of pebbles, USGS-Technical report, https://doi.org/10.3133/b730C, 1923.

Wentworth, C. K.: The Shapes of Rock Particles: A Discussion, The Journal of Geology, 41, 306–309, http://www.jstor.org/stable/30058840, 1933.

Williams, R. M. E., Grotzinger, J. P., Dietrich, W. E., Gupta, S., Sumner, D. Y., Wiens, R. C., Mangold, N., Malin, M. C., Edgett, K. S.,
620   Maurice, S., Forni, O., Gasnault, O., Ollila, A., Newsom, H. E., Dromart, G., Palucis, M. C., Yingst, R. A., Anderson, R. B., Herkenhoff,
         K. E., Le Mouélic, S., Goetz, W., Madsen, M. B., Koefoed, A., Jensen, J. K., Bridges, J. C., Schwenzer, S. P., Lewis, K. W., Stack, K. M.,
         Rubin, D., Kah, L. C., Bell, J. F., Farmer, J. D., Sullivan, R., Van Beek, T., Blaney, D. L., Pariser, O., Deen, R. G., null, n., Kemppinen,
         O., Bridges, N., Johnson, J. R., Minitti, M., Cremers, D., Edgar, L., Godber, A., Wadhwa, M., Wellington, D., McEwan, I., Newman, C.,
         Richardson, M., Charpentier, A., Peret, L., King, P., Blank, J., Weigle, G., Schmidt, M., Li, S., Milliken, R., Robertson, K., Sun, V., Baker,
625   M., Edwards, C., Ehlmann, B., Farley, K., Griffes, J., Miller, H., Newcombe, M., Pilorget, C., Rice, M., Siebach, K., Stolper, E., Brunet,
         C., Hipkin, V., Léveillé, R., Marchand, G., Sobrón Sánchez, P., Favot, L., Cody, G., Steele, A., Flückiger, L., Lees, D., Nefian, A., Martin,
         M., Gailhanou, M., Westall, F., Israël, G., Agard, C., Baroukh, J., Donny, C., Gaboriaud, A., Guillemot, P., Lafaille, V., Lorigny, E., Paillet,
         A., Pérez, R., Saccoccio, M., Yana, C., Aparicio, C. A., Caride Rodríguez, J., Carrasco Blázquez, I., et al.: Martian Fluvial Conglomerates
         at Gale Crater, Science, 340, 1068–1072, https://doi.org/10.1126/science.1237317, 2013.

630 Yingst, R. A., Crumpler, L., Farrand, W. H., Li, R., Cabrol, N. A., and Neakrase, L. D.: Morphology and texture of particles along the Spirit
         rover traverse from sol 450 to sol 745, Journal of Geophysical Research: Planets, 113, https://doi.org/10.1029/2008JE003179, 2008.

     Yingst, R. A., Cropper, K., Gupta, S., Kah, L. C., Williams, R. M. E., Blank, J., Calef, F., Hamilton, V. E., Lewis, K., Shechet, J., McBride,
         M., Bridges, N., Frias, J. M., and Newsom, H.: Characteristics of pebble and cobble-sized clasts along the Curiosity rover traverse from sol
         100 to 750: Terrain types, potential sources, and transport mechanisms, Icarus, 280, 72–92, https://doi.org/10.1016/j.icarus.2016.03.001,
635   2016.

     Yoshida, M. and Igarashi, Y.: Neogene to Quaternary lacustrine sediments in the Kathmandu Valley, Nepal, Journal of Nepal Geological
         Society, 1, 73–100, 1984.

     Zaheer, M., Khan, M. R., Mughal, M. S., Janjuhah, H. T., Makri, P., and Kontakiotis, G.: Petrography and Lithofacies of the Siwalik Group
         in the Core of Hazara-Kashmir Syntaxis: Implications for Middle Stage Himalayan Orogeny and Paleoclimatic Conditions, Minerals, 12,
640   https://doi.org/10.3390/min12081055, 2022.